Performance Projection of Electro-Optical Modulators for Radio-Over-Fiber in 2 GHz Cryogenic Front-End Receivers

Oscar Menéndez, Carlos Collado, Jordi Mateu, María C. Santos, and Juan M. O'Callaghan

***Abstract*—We present the design of a Y-Ba-Cu-O on $LiNbO_3$ cryogenic electro-optical modulator for analog 2 GHz applications. A resonant configuration of coplanar electrodes is considered, showing improvements with respect to both resonant Au electrodes and to traveling-wave electrodes, even beyond the traveling-wave theoretical maximum performance limit. The optimized layout is presented featuring a reduced length of 8.26 mm.**

***Index Terms*—Coplanar waveguide, high temperature superconductor, $LiNbO_3$, Mach-Zehnder electro-optical modulator, resonance.**

I. Introduction

WIRELESS communication services in the 2 GHz band are presently a subject of active research. Operation at cryogenic temperatures in conjunction with high temperature superconductors has proved the potential to increase performance in front-end receivers in this frequency band [1]. Using coplanar technology, Mach-Zehnder electro-optical modulators on $LiNbO_3$ (LNO) substrates have been successfully used to intensity modulate the radio-frequency signal into the optical carrier [2]; The most common configuration is traveling-wave (TW) modulators based on co-propagation of both waves. Cumulative phase shift acquired by the optical carrier over the interaction length is strongly dependent on the mismatch in propagating velocities and on the electrode loss, yielding a trade-off between usable bandwidth and maximum electrode length that in turns limits the maximum modulation efficiency for each given operation frequency. Several techniques have been reported to reduce and practically eliminate the velocities mismatch, and superconductors can be used to mitigate the effect of loss [3], [4], but still, technological constraints limit the interaction length and therefore the modulation efficiency in presently available electro-optical substrate samples.

Resonant modulators benefit from field enhancement at the resonance frequency that allows a reduction of the electrical feeding requirements with shorter electrode lengths, perfectly fitting into state-of-the-art electro-optical substrate samples. They feature a pass-band frequency characteristic better suited to narrow-band wireless applications than the broadband low-pass of TW modulators. It has been shown that they present less stringent conditions to the velocities mismatch and that their modulation efficiency is basically inversely proportional to the square root of loss, which makes operation at cryogenic temperatures and the use of superconductors specially interesting [5].

We present here the design of a resonant electro-optical modulator for operation in a cryogenic front-end receiver in the 2 GHz band. Y-Ba-Cu-O (YBCO) thin films deposited on a LNO substrate such as those obtained following the procedure in [6] are considered. The design is based on a resonant configuration consisting of an open-ended line of quarter wavelength at the operation frequency plus a feeding network connected to its midpoint. Coplanar line cross section parameters have been optimized to yield maximum performance. Predicted performance of this resonant modulator using conventional Au electrodes and of traveling-wave modulators are also presented for comparison.

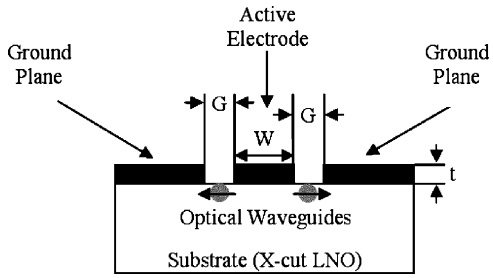

Fig. 1. Typical Mach-Zehnder modulator cross section using coplanar technology, which is defined by the active electrode width W and the inter-electrode gap G.

II. Modulator Design

A. General Considerations

Fig. 1 shows the geometry under consideration. A coplanar waveguide electro-optically induces optical phase shifts with the same magnitude but opposite signs onto the optical signals traveling through each of the optical waveguide arms of the integrated Mach-Zehnder interferometer. The longitudinal distribution of voltage between the active electrode and each ground plane is conveniently described by the equivalent electrical circuit model shown in Fig. 2. This circuit consists of a low-loss transmission line, a feeding network and two generic complex loads, which represent the reflective boundaries at each

Manuscript received October 4, 2004. This work was supported by the Spanish Ministry of Science and Technology under Project MAT2002-04551-C03-03 and by Generalitat de Catalunya (DURSI) under Grant 2001 SGR 0026.

O. Menéndez, C. Collado, M. C. Santos, and J. M. O'Callaghan are with the Universitat Politècnica de Catalunya (UPC), Campus Nord, UPC, Barcelona-08034 Spain (e-mail: joano@tsc.upc.es).

J. Mateu is with the CTTC—Centre Tecnològic de Telecomunicacions de Catalunya (e-mail: jordi.mateu@cttc.es).

Digital Object Identifier 10.1109/TASC.2005.850121

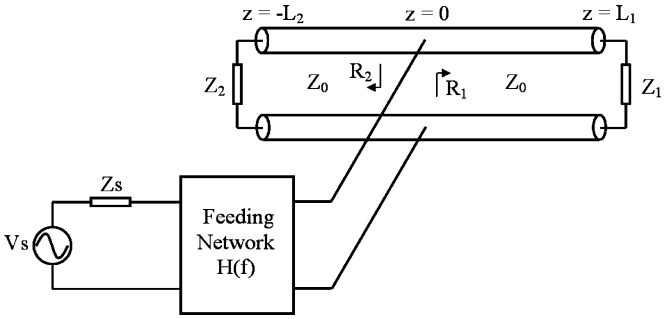

Fig. 2. Resonant modulator equivalent electrical circuit model, which consists of two generic complex loads, a low-loss transmission line and a feeding network.

end of the coplanar line. The reflected waves interfere with the incoming signal from the source causing at resonance an electric field enhancement that allows better modulation efficiencies. At this resonance frequency, the feeding network provides impedance matching to the source, so that all its available power is transferred to the transmission line, i.e. critical coupling.

Following the scheme on Fig. 2, for photons incident at time $t = t_0$ at the position $z = -L_2$, the difference of induced phase shifts into each optical waveguide over an interaction length $L = L_1 + L_2$ is given by [2]

$$\Delta\Phi(t_0) = -\frac{2\pi n_0^3 r\Gamma}{\lambda_0 G}\int_{-L_2}^{L_1} v\left(z, t_0 + \frac{n_0 z}{c}\right) dz \qquad (1)$$

where λ_0 is the optical wavelength, n_0 the optical refractive index, r the electro-optical coefficient, Γ the optical-electrical mode field overlap integral, G the inter-electrode gap and $v(z,t)$ is the instantaneous longitudinal distribution of voltage along the electrode which, as usual, can also be represented by its frequency dependent complex amplitude $V(z,f)$ by using Fourier decomposition,

$$v(z,t) = Re\left[\int_{-\infty}^{\infty} V(z,f)e^{j2\pi ft}df\right] \qquad (2)$$

where f is the modulating frequency. Applying standard microwave transmission line theory [7] over the equivalent circuit of Fig. 2 one gets

$$V(z,f) = \begin{cases} \frac{V}{1+R_1}\left[e^{-(\alpha+j\beta)z} + R_1 e^{(\alpha+j\beta)z}\right] & z \in \{0, L_1\} \\ \frac{V}{1+R_2}\left[R_2 e^{-(\alpha+j\beta)z} + e^{(\alpha+j\beta)z}\right] & z \in \{-L_2, 0\} \end{cases} \qquad (3)$$

where α and β are, respectively, the total loss per unit length, in Np/m, and the phase constant, R_1 and R_2 are the reflection coefficients to the right and to the left at the feeding point $z = 0$. V is the voltage at $z = 0$, which is related to the source voltage V_s through the feeding network transference function $H(f)$, $V = H(f)V_s$, which depends on the transmission line input impedance at $z = 0$, on the source impedance Z_s and on how the feeding network is implemented.

It is important to remark that the modulus of the induced phase shift $|\Delta\Phi(t_0)|$ determines the intensity modulation of the optical wave and hence all information regarding its phase may be discarded.

To assess the modulator performance for narrow-band wireless applications envisioned here, in a first approach, it is enough to find $|\Delta\Phi(t_0)|$ at the resonance frequency f_r. Modulator performance is evaluated from the source available power, P_π, required at f_r to cancel out the modulated output, i.e. $|\Delta\Phi_{f_r}| = |\Delta\Phi(t_0)|_{f=f_r} = \pi$. At this frequency, if we assume critical coupling, $H(f_r)$ is independent of how the feeding network is implemented, and we can write

$$V = V_s \frac{\sqrt{\frac{R_{in}}{Z_s}}}{2 - j\frac{2X_{in}}{Z_{in}}} \qquad (4)$$

where Z_{in} is the transmission line input impedance at $z = 0$ at f_r, and R_{in} and X_{in} are, respectively, the real and imaginary parts of Z_{in}, which are related to the transmission line length (L_1, L_2), to the complex loads (Z_1, Z_2) and to the transmission line electrical parameters, i.e. total loss per unit length (α), characteristic impedance (Z_0) and electrical refractive index (n_e).

B. Resonant Topology Under Consideration

Following the analysis outlined in the previous section we have carried out a study of performance versus length, at 2 GHz, for a variety of modulators with different resonant topologies all described generically by the scheme in Fig. 2 [5]. As a result, we have found that the open-ended $L = \lambda_e/4$ line fed through its midpoint $(L_1 = L_2 = \lambda_e/8)$ by the appropriate feeding network presents a good trade-off. Therefore we choose it as our basic design configuration. Note that the electrode length L is given in terms of the electrical wavelength at the resonance frequency, i.e. $\lambda_e = c/f_r n_e$, where c is the vacuum light velocity.

The substrate of choice is X-cut LNO, on which YBCO thin films with good microwave properties can be grown [6]. Deposited YBCO has a thickness $t = 230$ nm and its measured surface resistance R_s is about 0.7 mΩ at 65 K and 8 GHz, while LNO has an electrical permittivity $\varepsilon_r = 34.7$, an optical refractive index $n_0 = 2.2$ and a loss tangent $tan\delta = 0.002$ at 65 K.

Taking into account that the total loss per unit length (α) consists of electrode plus dielectric loss, and that the electrode loss is proportional to the surface resistance R_s [8], [9], we assume the frequency dependence of the total loss to be given by

$$\alpha(f) = \alpha_e \cdot f^2 + \alpha_d \cdot f \qquad (5)$$

where α_e and α_d are proportionality constants for electrode and dielectric loss respectively.

It can be shown that the main effect of loss, for the typical loss values, is a reduction in the maximum peak voltage in the line, whereas the voltage distribution along the line can be assimilated to that calculated neglecting the loss effect [5]. Using this and (1)–(5), we can write the induced phase shift at f_r as

$$|\Delta\Phi_{f_r}| = V_s\sqrt{\frac{\lambda_{e0}}{Z_s\lambda_0^2}}r\frac{Z_0^{\frac{1}{2}}\Gamma}{\alpha^{\frac{1}{2}}G}\frac{n_0 n_e^{\frac{3}{2}}\left[-\sqrt{2} + 2\frac{n_0}{n_e}sin\left(\frac{\pi}{4}\frac{n_0}{n_e}\right)\right]}{1 - \left(\frac{n_e}{n_0}\right)^2} \qquad (6)$$

where $\lambda_{e0} = c/f_r$ is the vacuum electrical wavelength.

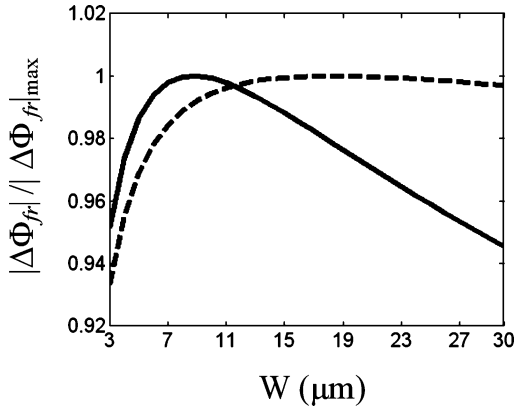

Fig. 3. Normalized induced phase shift at the resonance frequency (2 GHz) as a function of W. Continuous line represents the YBCO resonant modulator with $G = 15\ \mu\mathrm{m}$, whereas dashed line represents the same resonant configuration but with Au electrodes at cryogenic temperature.

This closed-form expression helps to identify the main dependences and parameters to optimize through proper design of the modulator. From (6) we see that, for a given V_s, $|\Delta\Phi_{f_r}|$ consists of 2 terms.

First term is $\sqrt{(\lambda_{e0}/Z_s\lambda_0^2)}r$, which depends exclusively on parameters not susceptible to optimization. In our case we consider $f_r = 2$ GHz, the third optical spectral window $\lambda_0 = 1550\ \mathrm{nm}$ and the source impedance is taken to be $Z_s = 50\ \Omega$. The electro-optical coefficient, r, depends on the electro-optical substrate under consideration (LNO) and the orientations of the electric field vectors of the modulating and the optical waves relative to the substrate. In the case of LNO they are all taken to follow the direction of the optical axis to address the highest possible element in the electro-optical tensor $r_{33} = 30.8\,\mathrm{pm/V}$. In our X-cut substrate that means arranging the optical waveguides as shown in Fig. 1 and launching the optical signal linearly polarized in the optical TM mode.

The second term, $(Z_0^{1/2}\Gamma/\alpha^{1/2}G)(n_0n_e^{3/2}[-\sqrt{2}+2(n_0/n_e)sin((\pi/4)(n_0/n_e)])/(1-(n_e/n_0)^2)$, only depends on the cross section geometry of the modulator, and we will refer it as *cross section term* in the next section.

C. Cross Section Term Optimization

Coplanar line cross section is basically defined through two parameters, see Fig. 1, the active electrode width W and the inter-electrode gap G. We fix G to 15 μm, which is a typical choice balancing high Γ and ease of fabrication [8], and W will be chosen to maximize the cross section term. W will basically affect the value of Z_0/α and also in a less important way the value of n_e, whereas we can consider that the value of Γ/G won't change. Using (6), we get induced phase shift at the resonance frequency (2 GHz) as a function of W (Fig. 3). The optimum W is about 9 μm which is a technologically viable value, therefore we take $W = 9\ \mu\mathrm{m}$ in our design but we note that the active electrode width is not a critical design parameter in the range shown in Fig. 3.

Table I shows the length and electrical parameters at the resonance frequency (2 GHz) for a modulator designed with $G = 15\ \mu\mathrm{m}$ and $W = 9\ \mu\mathrm{m}$. These parameters have been obtained following the procedure described in [9].

TABLE I
ELECTRICAL PARAMETERS AT 2 GHz AND LENGTH FOR A YBCO MODULATOR DESIGNED WITH $G = 15\ \mu\mathrm{m}$ AND $W = 9\ \mu\mathrm{m}$

Z_0 (Ω)	45.78
α_e (dB/m)	1.93
α_d (dB/m)	1.60
n_e	4.54
L (mm)	8.26

TABLE II
PREDICTED PERFORMANCE COMPARISON

	YBCO	TW-Limit	Au(65 K)	Au	Com. TW
P_π (mW)	2.4	5	35	80	60-120

III. PROJECTED PERFORMANCE EVALUATION

Here we present predicted performance results of the YBCO modulator designed in the last section. Projected performance of the same resonant configuration using Au electrodes and TW modulators are also discussed for comparison. As we have explained previously, modulator performance is evaluated using the source available power necessary to reach $|\Delta\Phi_{f_r}| = \pi$ at 2 GHz, i.e. P_π.

From (6), we obtain that the YBCO modulator has a P_π of 2.4 mW, using data of Table I, and $\Gamma = 0.61$ calculated using [10], [11].

Following the same analysis used in the previous sections, we design a resonant modulator with Au electrodes at cryogenic temperature. If we assume gold conductivity is $2 \times 10^8\ \mathrm{S/m}$ at 65 K, $t = 5\ \mu\mathrm{m}$ and $G = 15\,\mu\mathrm{m}$, then the optimum W is 18 μm (Fig. 3). From this figure, it is obvious that W choice is not a critical decision, then we can use $W = 9\ \mu\mathrm{m}$, which we used in the YBCO modulator design, without loosing much modulation efficiency. For this case, P_π is about 35 mW. If this Au resonant modulator is used at room temperature, its P_π is about 80 mW.

Commercial TW modulators have a P_π about 60–120 mW for applications at 2 GHz. TW theoretical maximum performance limit (TW-Limit) considers the ideal case where there is no mismatch in velocities, lossless, $\Gamma = 1$ and the modulator length is limited by the sample size ($\sim$5 cm). In this case, using $G = 15\ \mu\mathrm{m}$, P_π is about 5 mW.

Table II is a summary of predicted performance at 2 GHz. We can observe that cryogenic resonant modulators have a lower P_π than commercial TW modulators, and in the case of the YBCO resonant modulator its P_π is even lower than the TW theoretical maximum performance limit. The Au resonant modulator at room temperature has a P_π comparable with commercial TW modulators but with a much shorter length.

Fig. 4 shows $|\Delta\Phi(t_0)|$ as a function of frequency of the YBCO modulator. The modulator bandwidth is about 10 MHz. It is important to remark that reducing the value of α causes an unloaded quality factor increase which narrows the operative bandwidth around the resonance frequency, therefore it is very important to check the modulator bandwidth to know if it is suitable to our application.

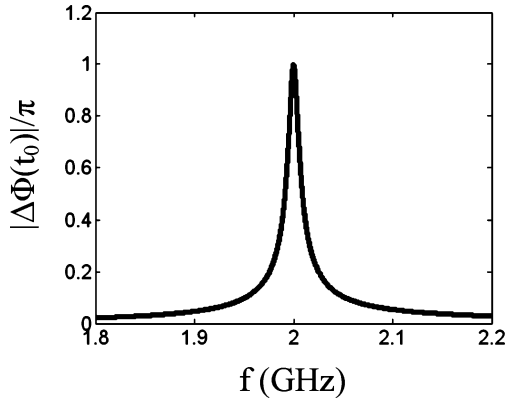

Fig. 4. Induced phase shift as a function of frequency of the YBCO modulator ($G = 15\ \mu\mathrm{m}$ and $W = 9\ \mu\mathrm{m}$).

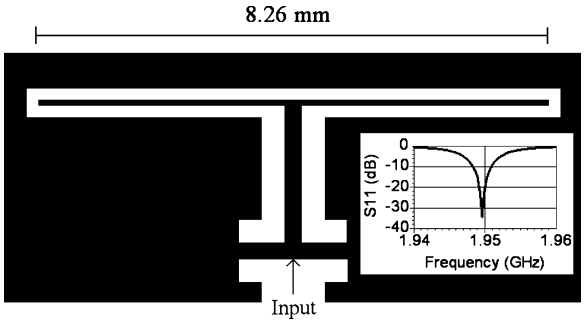

Fig. 5. Modulator layout.

Fig. 5 shows the layout of the YBCO modulator designed in this work. The modulator active region has a length of 8.26 mm, with an active electrode width of 9 μm and an inter-electrode gap of 15 μm. The feeding network, designed to achieve critical coupling at 2 GHz, consists of a stub, whose length is 2.16 mm, ended in two short-ended stubs in parallel. Each short-ended stub has a length of 0.49 mm. This feeding network is designed with coplanar technology with an active electrode width of 20 μm and an inter-electrode gap of 55 μm. With this cross section, its electrical parameters at 2 GHz are: $Z_0 \simeq 50\ \Omega$, $n_e = 4.28$, $\alpha_e = 0.83\,\mathrm{dB/m}$ and $\alpha_d = 1.51\,\mathrm{dB/m}$. The inset shows the electromagnetic simulation [12], where we notice that there is a reflection coefficient of about -32 dB at the resonance frequency.

IV. Conclusions

In this work we have presented the design of a Mach-Zehnder electro-optical resonant modulator based on coplanar YBCO thin films on a LNO substrate for narrow-band wireless applications in the 2 GHz band. This modulator exploits the resonance condition in the active electrode to achieve low power operation compared with TW modulators and with a much shorter length.

We have derived a closed-form expression for the induced phase shift, which allows to obtain the optimum modulator design. Predicted performance analysis yields a source available power P_π of about 2.4 mW in a 8.26 mm electrode length. The bandwidth of this modulator is about 10 MHz around 2 GHz.

Resonant modulators are thus promising for use in distributed antenna systems where the electrical signal is directly sent over an optical carrier through optical fiber to the remote antenna units. Its reduced size and low power consumption could simplify the drivers needed, and could allow integration of several modulators in a single substrate chip.

References

[1] R. R. Mansour, "Microwave superconductivity," *IEEE Trans. Micro. Theory Tech.*, vol. 50, no. 3, pp. 750–759, 2002.
[2] R. C. Alferness, "Waveguide electrooptic modulators," *IEEE Trans. Micro. Theory Tech.*, vol. 82, no. 8, pp. 1121–1137, 1982.
[3] K. Yoshida, Y. Kanda, and S. Kohjiro, "A travelling-wave-type $\mathrm{LiNbO_3}$ optical modulator with superconducting electrodes," *IEEE Trans. Micro. Theory Tech.*, vol. 47, no. 7, pp. 1201–1205, 1999.
[4] E. Rozan, C. Collado, A. Garcia, J. M. O'Callaghan, R. Pous, L. Fabrega, J. Rius, R. Rubi, J. Fontcuberta, and F. Harackiewicz, "Design and fabrication of coplanar YBCO structures on lithium niobate substrates," *IEEE Trans. Appl. Supercond.*, vol. 9, no. 2, pp. 2866–2869, 1999.
[5] C. Collado, O. Menéndez, M. C. Santos, J. Mateu, and J. M. O'Callaghan, "General equations for the induced phase shift in resonant electro-optic modulators," *IEEE Photon. Technol. Lett.*, to be published.
[6] L. Fabrega, R. Rubi, J. Fontcuberta, F. Sanchez, C. Ferrater, M. V. Garcia-Cuenca, M. Varela, C. Collado, J. Mateu, O. Menéndez, and J. M. O'Callaghan, "Reduced microwave losses of YBCO thin films on electro-optic $\mathrm{LiNbO_3}$ crystals," *J. Appl. Phys.*, vol. 92, no. 10, pp. 6346–6348, 2002.
[7] D. Pozar, *Microwave Engineering*: John Wiley & Sons, Inc., 1998.
[8] K. Noguchi, H. Miyazawa, and O. Mitomi, "75 GHz broadband $\mathrm{Ti:LiNbO_3}$ optical modulator with ridge structure," *Electron. Lett.*, vol. 30, no. 12, pp. 949–950, 1994.
[9] D. M. Sheen, S. M. Ali, D. E. Oates, R. S. Withers, and J. A. Kong, "Current distribution, resistance, and inductance for superconducting strip transmission lines," *IEEE Trans. Appl. Supercond.*, vol. 1, no. 2, pp. 108–115, 1991.
[10] Z. Xiang and T. Miyoshi, "Optimum design of coplanar waveguide for $\mathrm{LiNbO_3}$ optical modulator," *IEEE Trans. Micro. Theory Tech.*, vol. 43, no. 3, pp. 523–528, 1995.
[11] Ansoft HFSS version 3.0.21, Ansoft Corporation.
[12] Advanced Design System 2002, Agilent Technologies.